



Available online at www.sciencedirect.com

ScienceDirect

Geochimica et Cosmochimica Acta 223 (2018) 216-228

Geochimica et Cosmochimica Acta

www.elsevier.com/locate/gca

Aqueous magnesium as an environmental selection pressure in the evolution of phospholipid membranes on early earth

Punam Dalai^a, Putu Ustriyana^a, Nita Sahai^{a,b,c,*}

Received 25 July 2017; accepted in revised form 30 November 2017; available online 8 December 2017

Abstract

Early compartmentalization of simple biomolecules by membrane bilayers was, presumably, a critical step in the emergence of the first cell-like entities, protocells. Their membranes were likely composed of single chain amphiphiles (SCAs), but pure SCA membranes especially those with short-chains are highly unstable towards divalent cations, which are ubiquitous in aqueous environments. The prebiotic synthesis of phospholipids (PLs), even in only trace amounts, may also have been possible. PL membranes are much more stable towards divalent cations. Here, we show the transition of fatty acid membranes to mixed fatty acid-PL and, finally, to PL membranes in the presence of Mg^{2+} , which acts as an environmental selection pressure, and we propose different mechanisms for the observed increased Mg^{2+} -immunity. The "fatal" concentration ([Mg²⁺]_{fatal}) at which vesicles are disrupted increased dramatically by an order of magnitude from OA to mixed to POPC vesicles. Two mechanisms for the increasing immunity were determined. The negative charge density of the vesicles decreased with increasing POPC content, so more Mg^{2+} was required for disruption. More interestingly, Mg^{2+} preferentially bound to and abstracted OA from mixed lipid membranes, resulting in relatively POPC-enriched vesicles compared to the initial ratio. The effect was the most dramatic for the largest initial OA-POPC ratio representing the most primitive protocells. Thus, Mg^{2+} acted to evolve the mixed membrane composition towards PL enrichment. To the best of our knowledge, this is the first report of selective lipid abstraction from mixed SCA-PL vesicles. These results may hold implications for accommodating prebiotic Mg^{2+} -promoted processes such as non-enzymatic RNA polymerization on early Earth. © 2017 Elsevier Ltd. All rights reserved.

Keywords: Fatty acid; Phospholipid; Magnesium; Fatal concentration; Protocell

1. INTRODUCTION

The most fundamental requirement for the origin of life was the emergence of a self-assembling molecular system capable of both metabolism and replication. The earliest self-assembling life-like unit, the protocell, was likely an enclosed entity that protected genetic and metabolic molecules from degradation by conditions in the external envi-

E-mail address: sahai@uakron.edu (N. Sahai).

ronment. It has been assumed that protocell membranes were composed of single chain ampiphiles (SCAs) such as fatty acids, fatty alcohols, monoalkyl phosphates and monoacyl glycerol phosphate esters, because of their prebiotic availability and ability to self-assemble into bilayer structures (Deamer and Oró, 1980; Oró et al., 1990; Apel et al., 2002; Monnard and Deamer, 2002; Mansy et al., 2008; Budin et al., 2012; Adamala and Szostak, 2013; Albertsen et al., 2014; Dalai et al., 2016; Kee and Monnard, 2016; Fiore et al., 2017). In particular, various SCAs (up to C₁₂) and polyaromatic hydrocarbons have been discovered in carbonaceous chondrites (Yuen and Kvenvolden, 1973; Lawless and Yuen, 1979; Deamer and

^a Department of Polymer Science, 170 University Avenue, University of Akron, Akron, OH 44325-3909, United States
^b Department of Geosciences, 170 University Avenue, University of Akron, Akron, OH 44325-3909, United States

c Integrated Bioscience Program, 170 University Avenue, University of Akron, Akron, OH 44325-3909, United States

^{*} Corresponding author at: Department of Polymer Science, 170 University Avenue, University of Akron, Akron, OH 44325-3909, United States.

Pashley, 1989; Komiya et al., 1993; Mautner et al., 1995; Monnard and Deamer, 2002), and fatty acids up to C₂₂ were formed via Fisher-Tropsch type (FTT) synthesis under simulated hydrothermal conditions (Nooner and Oró, 1979; McCollom et al., 1999; Rushdi and Simoneit, 2001; Foustoukos, 2004).

Single chain amphiphile membranes are capable of encapsulating and concentrating the building blocks of life, self-division and are thermostable up to ~ 90 °C (Monnard and Deamer, 2002; Mansy and Szostak, 2008). A key step in energy transduction is nutrient uptake and release of waste products across the membrane. Fatty acid membranes are reported to be permeable towards sugars (Gebicki and Hicks, 1976; Hargreaves and Deamer, 1978; Sacerdote and Szostak, 2005), amino acids (Zepik et al., 2007) and nucleic acids (Mansy et al., 2008). However, one of the major limitations of fatty acid membranes is their instability in the presence of salts (Monnard and Deamer, 2002; Monnard et al., 2002). Modern seawater contains ~ 500 mM NaCl and over 50 mM Mg²⁺ among other ions (Berner and Berner, 2012). The dissolution of minerals from komatiite, the rock comprising ancient oceanic crust, and tonalite, representing primitive continentaltype crust would have resulted in dissolved salts in Hadean-Archean aqueous environments. Evaporation of post-weathering solutions would have resulted in even higher salt concentrations with estimates of $\sim 600 \text{ mM}$ NaCl, ~ 0.1 to 10 mM of total dissolved magnesium and sub-millimolar levels of dissolved calcium. Fatty acid vesicles are disrupted at modest (<1 mM) divalent and moderate $(\sim 200 \text{ mM})$ monovalent cation concentrations (Monnard et al., 2002; Chen et al., 2005). The instability of pure fatty acid membranes towards divalent cations has posed a significant constraint on studies of model protocellular membranes under plausible prebiotic conditions.

Mixed vesicles of fatty acids with fatty alcohols, fatty amines, glycerol monodecanoate or polycyclic aromatic hydrocarbons are more tolerant of divalent cations (Hargreaves and Deamer, 1978; Deamer, 1992; Apel et al., 2002; Chen et al., 2005; Mansy et al., 2008; Namani and Deamer, 2008; Groen et al., 2012; Adamala and Szostak, 2013). Recently, it has been reported that nucleobases and sugars prevent the aggregation of decanoic acid (DA) and stabilize it in 300 mM NaCl (Black et al., 2013). Thus, mixed SCA vesicles are more likely to have been stable in salt-rich environments.

In contrast to SCA membranes, the phospholipid (PL) membranes of modern cells are almost impermeable to most solutes and, therefore, need specialized transport machineries for nutrient exchange, and these ion channels or pumps likely evolved later than the emergence of the first protocells. The transition of protocell membranes composed predominantly of fatty acid or mixed SCA membranes to PL membranes would, presumably, have been a necessary step to compensate the limitations associated with both fatty acid and PL systems. The prebiotic synthesis of PLs, even if only in trace amounts, may have been possible (Hargreaves et al., 1977; Rao et al., 1982, 1987; Maheen et al., 2010; Patel et al., 2015), so an intermediate evolutionary stage in which protocell membranes were

composed of mixed fatty acid-PL vesicles is envisaged. Following this logic, previous studies examined fatty acid-PL vesicles, but in the absence of divalent cations (e.g., Cheng and Luisi, 2003; Budin and Szostak, 2011). It was shown that mixed vesicles of oleic acid (OA) and 1-palmi toyl-2-oleoylphosphatidylcholine (POPC) or of OA and di-oleoyl-phosphatidic acid (DOPA) grow at the expense of pure OA vesicles. However, the resulting vesicles should be relatively more OA-enriched than the starting population and, hence, less stable towards divalent cations, so the evolutionary advantage is not immediately apparent.

Among the divalent ions, Mg²⁺ is one of the most important biologically because it is required at relatively high (50-80 mM) concentrations for both nonenzymatic templated polymerization of RNA nucleotides and nonenzymatic clay-catalyzed nucleotide polymerization (Ferris et al., 1996; Joshi et al., 2009; Adamala and Szostak, 2013). It is important to note, however, that Mg²⁺ is not essential for the formation of short RNA oligomers as long as specifically pre-treated montmorillonite and a high concentration of monovalent alkali cations are present (Joshi and Aldersley, 2013). Also, it has been shown that Fe²⁺ can catalyze single-electron transfer reactions by ribosomal RNA in the absence of oxygen and at mildly acidic pH (Hsiao et al., 2013). Long chain RNA oligomerization, however, does seem to require high Mg²⁺ concentrations and Fe²⁺ may also have a deleterious effect on primitive membranes, so it is critical to understand the stability of protocell membranes and their transition to PL membranes in the presence of divalent cations, especially, high Mg²⁺ concentrations.

Given the key role of Mg²⁺ in protocell evolution, the aim of the present work is to quantitatively investigate the Mg-tolerance of vesicles composed of binary mixtures of OA and POPC as model protocell membranes (Fig. 1) and the mechanisms responsible for the increasing Mgtolerance as membrane composition changes towards PLs. In so doing, the role of Mg^{2+} in acting as an environmental selection pressure in the transition of fatty acid membranes to mixed fatty acid-PL membranes and, finally, to PL membranes has been revealed. As noted above, membranes composed of DA and decanol (DOH) have been widely examined as the earliest model protocell membranes by some workers (e.g., Apel et al., 2002; Monnard and Deamer, 2002; Sahai et al., 2017). To determine whether the effects of Mg²⁺ obtained here on OA-POPC vesicles are more broadly applicable, we also examined the effects of Mg²⁺ and Ca²⁺ on mixed DA-DOH (1:1 and 2:1) vesicles. To the best of our knowledge, this is the first report on the evolution of fatty acid membranes towards PL membranes driven by an ion.

2. MATERIALS AND METHODS

Oleic acid (C18:1, OA) and 1-palmitoyl-2-oleoyl-sn-glycero-3-phosphocholine (C16:0-C18:1, POPC) were obtained from Avanti[®] Polar Lipids (Alabaster, AL, USA). Unless otherwise specified, all other chemicals were purchased from Sigma-Aldrich (St. Louis, MO, USA) at the highest available purity, and used without further

Fig. 1. Structures of (A) OA and (B) POPC.

purification. All solutions were prepared with ultrapure deionized water with a resistivity of $18.2 \text{ M}\Omega \cdot \text{cm}$ (BarnsteadTM GenPureTM xCAD Plus, Thermo Scientific, Rockford, IL, USA).

2.1. Vesicle preparation

Stock solutions of 10 mM OA (pKa = 9.85, CVC = 0.02-0.2 mM), OA-POPC (10:1, 5:1, 3:1, and 1:1), POPC $(CVC = \le 0.025 \,\mu\text{M})$ were prepared separately by dissolving lipids in chloroform. Organic solvent was removed with a stream of N₂ to form a thin lipid film. Samples were then kept in a vacuum desiccator for 3-4 h to completely remove chloroform. Afterwards, thin lipid films were rehydrated with bicine buffer (200 mM, pH 8.5) to form a 10 mM stock of vesicles and then sonicated for ~ 1 min. All vesicle stock solutions were gently agitated by end-over-end rotation overnight prior to use in order to ensure that the vesicles remain stable. The presence of vesicles in all OA, OA-POPC, and POPC systems was supported by measuring the particle size by dynamic light scattering (DLS) size measurements and confirmed by phase contrast light microscopy. In a separate experiment, 50 mM DA-DOH (2:1, 1:1) vesicle stock was prepared in bicine buffer (200 mM, pH 8.5) to compare the results obtained for mixed OA-POPC systems.

2.2. Determination of fatal ion concentration

2.2.1. Fluorescence assay

Magnesium tolerance was estimated by defining the term, fatal magnesium concentration ([Mg2+]fatal), which is the amount of Mg²⁺ that ruptures a majority of vesicles. The fatal ion concentration ($[Mg^{2+}]_{fatal}$) to vesicle bilayers was determined by naphtho[2,3-a]pyrene (NP) fluorescence assay. Previous studies have used the hydrophobic dye, pyrene, to indicate the presence of vesicles (Vanderkooi and Callis, 1974; Almgren et al., 1979; Schenkman et al., 1981; Chen and Szostak, 2004a,b; Chen et al., 2005). In this study, NP (Molecular Probes, Eugene, OR, USA), a membrane-soluble dye was used as an indicator for the presence of intact bilayer membranes. When vesicles form, NP is concentrated in the lipid bilayer as dimers, known as "excimers," that is the state between excited and groundstate monomers (Fig. EA-1a). These dimers have peaks at 465 and 495 nm, respectively. The fluorescence of NP in micelle/monomer solutions is characterized by a strong

"monomer" emission at 390 nm and a negligible excimer peak (Fig. EA-1b). Note that NP may also get concentrated in lipid aggregates to form excimers that can exhibit fluorescence. The lipid aggregates, however, are usually larger in size than most of the vesicle population.

In detail, 0.1 mM NP stock was prepared by dissolving in chloroform and then dispatched into a quartz 96microwell plate to achieve a final concentration of 0.5 mol % NP relative to the lipid being investigated (Chen and Szostak, 2004a,b). The chloroform was evaporated in a vacuum desiccator for 30 min. Next, non-extruded lipid vesicle stock solution prepared as described above (see Section 2.1) and bicine buffer (200 mM, pH 8.5) were added to each well to adjust the volume to a final lipid concentration was 2 mM for all lipid systems (OA, mixed OA-POPC (10:1, 5:1, 3:1, 1:1, and POPC)). The total lipid concentration (2as kept low to minimize potentialmM) was kept low to minimize potential interference of vesicle turbidity on fluorescence. The plate was kept shaking (Open-Air Rocker, Fisher Scientific, Waltham, MA, USA) for 30 min for equilibration. Subsequently, different amounts of MgCl₂ were pipetted from a stock solution (50 mM) into the wellplates to have variable final MgCl₂ concentrations (0, 2.5, 5, 7.5, 10, 15, 20, 22.5, 25, 27.5, 30, 35, and 40 mM) and the plate was again placed on the rocker for 1 h. The final volume, after adding all vesicle stock, bicine buffer and MgCl₂ solution, was 250 μL. In some cases, high MgCl₂ concentrations (above 40 mM) were prepared from a 200 mM MgCl₂ stock. The samples were then analyzed with a Synergy H1 multi-mode plate reader (BioTek Instruments, Winooski, VT, USA) equipped with fluorescence spectroscopy. All samples were prepared in triplicate and the entire experiment was repeated twice.

To examine the effect of the vesicle size on the fluorescence, experiments were also performed with extruded vesicles passed 11 times through a 200 nm polycarbonate membrane using a mini-extruder (Avanti[®] Polar Lipids, Alabaster, AL, USA) to form homogenous, monodisperse, and single-bilayer vesicles (Fig. EA-1c).

2.2.2. DLS particle size assay

The [Mg²⁺]_{fatal} values for OA, mixed OA-POPC and POPC systems were also identified by DLS measurements. Vesicles were prepared as described in Section 2.1. The vesicle suspensions were subsequently extruded 11 times through a 200 nm polycarbonate membrane to form homogenous, monodisperse, and single-bilayer vesicles

(Fig. EA-2). The extruded vesicles were then equilibrated again for at least 1 h. The extruded vesicles in the various lipid systems were found to have a size range of 160–200 nm and this size was stable for at least up to 24 h.

Variable amounts of $MgCl_2$ were pipetted from a stock (50 mM) and each lipid system (total lipid concentration = 2 mM) in eppendorf tubes (1.5 mL) to achieve the final concentrations (0, 2.5, 5, 7.5, 10, 15, 20, 22.5, 25, 27.5, 30, 35, and 40 mM) of $MgCl_2$. The eppendorf tubes containing mixtures of lipid and $MgCl_2$ were allowed to equilibrate for 1 h with end-over-end rotation. In some cases, high $MgCl_2$ concentrations (above 40 mM) were prepared from a 200 mM $MgCl_2$ stock.

Aliquots of 400 µL were introduced into disposable semi-micro cuvettes (BrandTech, Brand GmbH, Wertheim, Germany) and DLS measurements were conducted at 25 °C using a ZetaSizer NanoSeries ZS preset with a backscattering angle of 173° (Malvern Instruments, London, UK). Particle size was determined one hour after addition of MgCl₂ at various concentrations. The average particle diameter (nm) of each sample serves as an indicator of lipid-Mg aggregation. The magnesium concentration at which the particle diameter began to increase beyond the baseline established by the 0 mM MgCl₂ sample was assigned as the $[Mg^{2+}]_{fatal}$. All experiments were conducted in triplicate and the entire experiment was repeated two times. The errors bars reflect the standard deviation of triplicate measurements. Other concentrations of OA and mixed OA-POPC (0.25, 0.5, and 1 mM) were also studied to examine effect of total lipid concentration on [Mg²⁺]_{fatal}.

2.2.3. Microscopy

Pure and mixed lipid systems were imaged with phase contrast light microscopy (Fig. EA-3). Two millimolar of OA, mixed OA-POPC or POPC vesicles prepared at pH 8.5 (bicine buffer, 200 mM) (see Section 2.1) were preequilibrated overnight prior to use before sampling into 1.5 mL microcentrifuge tubes. A variable amount of a concentrated MgCl₂ stock solution (50 mM) was added to the vesicle solutions to obtain a final MgCl₂ concentration ranging from 0 to 40 mM. After 1 h of the addition of MgCl₂ solution to the vesicles, the solution was pipetted onto a glass slide and viewed with an inverted microscope (Olympus IX51, Olympus America Inc., Melville, NY, USA) using a $100 \times \text{oil}$ objective lens. Images were recorded with an sCMOS camera (QImaging, optiMOS, Surrey, BC, Canada) and were viewed using a cellSens Dimension 1.7 software.

2.3. Calcein leakage assay

This assay is based on the permeability of encapsulated calcein, a water-soluble and self-quenching fluorescent dye, through various lipid membranes as a function of time and in the presence of different magnesium concentrations. Calcein was encapsulated in vesicles above its self-quenching concentration (>70 mM). The leakage of calcein results in its dilution in the extra-vesicular solution, which is measured as an increase in fluorescence and is reported as a percentage decrease in encapsulation.

OA, OA-POPC (10:1, 5:1, 3:1, and 1:1), and POPC were dissolved separately in chloroform. The solvent was removed using a stream of N₂ gas and the sample was then placed under vacuum for 3-4 h to ensure complete solvent evaporation. The lipid film was rehydrated with bicine buffer (200 mM, pH 8.5) and 20 mM calcein to achieve a final lipid concentration of 20 mM. After brief sonication (\sim 1 min), the samples were freeze-thawed five times to promote more vesicle formation and, hence, greater encapsulation of the dye. The samples were then allowed to equilibrate overnight. Samples were extruded 11 times through a 200 nm polycarbonate membrane using a miniextruder (Avanti® Polar Lipids, Alabaster, AL, USA) to form monodisperse and unilamellar vesicles. Calceinencapsulating vesicles were separated from the unencapsulated dye by size-exclusion chromatography. In detail, 350 µL of the sample were loaded in a glass column (20 cm × 1 cm) filled with Sephadex G-50 medium beads (Sigma Aldrich, St. Louis, MO, USA). The mobile phase used was a bicine buffer (200 mM) at pH 8.5. Fractions were collected (FC204 Fraction Collector, Gilson, Middleton, WI, USA) in a 96-microwell plate (6 drops/well) and the fluorescence was measured in a plate reader (Synergy H1, BioTek Instruments, Winooski, VT, USA) at Ex/Em wavelengths of 495/530 nm (Fig. EA-4a).

Vesicle fractions containing encapsulated calcein were mixed together. The total volume recovered was $\sim 3.5 \, \text{mL}$, resulting in a total lipid concentration of $\sim 2 \, \text{mM}$ after column purification. Subsequently, MgCl₂ (5–40 mM) dissolved in bicine buffer was added to the vesicles using a multichannel pipette and mixed in a 96-microwell plate to achieve a final volume of 200 μL . The addition of Triton TM-100X (1%, 4 μL) ruptures the vesicles immediately and, thus, the remaining encapsulated calcein leaks out, leading to maximum fluorescence intensity (maximum leakage or total vesicle rupture). Kinetics of calcein leakage were recorded in a plate reader every 15 s for 1.5–2 h. Each experiment was performed in duplicate and the entire experiment was repeated two times.

The percentage of encapsulation was calculated according to the equation

Encapsulation (%) =
$$100 \times \left(1 - \frac{F_t - F_0}{F_f - F_0}\right)$$
 (1)

where F_t is the fluorescence at time t, F_0 is the fluorescence at time zero, and F_f is the fluorescence after the addition of Triton. In practice, F_0 was taken as the fluorescence after five minutes to allow for any initial perturbances or variations introduced due to the time taken to pipette MgCl₂ solution into the microwells.

In Eq. (1) above, it is assumed that fluorescence intensity depends solely on concentration of calcein that has leaked out of the vesicle. In reality, other factors may also influence the fluorescence signal. First, we consider that calcein (-4 charge) which has leaked out may bind to extravesicular Mg²⁺. This causes a decrease in free calcein concentration, hence, a re-quenching and a decrease in fluorescence intensity is observed (Fig. EA-4b; Furry, 1985). The above equation does not account for such situations, so this effect would appear as an apparent increase in

encapsulation. Secondly, in the equation above, it is assumed that all the calcein was removed from the background (extra-vesicular) solution in the preceding column purification step before the addition of MgCl₂. If column separation is not optimal, residual calcein remaining in the extra-vesicular solution may bind to Mg²⁺ and this would also result in an apparent increase in encapsulation. Hence, obtaining good column separation is critical (e.g., Fig. EA-4a). A third factor that may influence fluorescence intensity change is if the vesicle size were to increase or decrease, due to osmolarity difference across the membrane. thus affecting the internal calcein concentration. In order to check whether vesicle size changes before and after exposure to Mg²⁺, we determined vesicle size by DLS where vesicles were prepared in the absence and presence of 0.1 M NaCl in the bicine buffer solution. The vesicle size remained approximately constant under all conditions (Table EA-1), suggesting that osmolarity differences did not affect the fluorescence signal in the calcein leakage experiments. In summary, the encapsulation calculated using Eq. (1) primarily provides an estimate of apparent calcein encapsulation and calcein-Mg binding in the extra-vesicular solution. Leakage experiments are not reported for DA-DOH because they are much more leaky than OA-POC vesicles and even the initial encapsulation of calcein is problematic.

2.4. Zeta (ζ) potential measurement

Ten millimolar stocks of OA, mixed OA-POPC, and POPC vesicles prepared in bicine buffer (200 mM, pH 8.5) were extruded 11 times through a 200 nm polycarbonate membrane. The extruded vesicle samples were allowed to equilibrate with 1 h by end-over-end rotation. Afterwards, aliquots of extruded vesicle stocks were diluted with bicine buffer (200 mM, pH 8.5) and 50 mM MgCl₂ stock in bicine buffer was added to reach a total lipid concentration of 2 mM and various concentrations of MgCl₂ (0, 2.5, 5, 10, 20, 30, and 40 mM). The entire system was again equilibrated for 1 h. Subsequently, a 500 µL sample was filtered using a centrifuge tube filter with a pore size of $0.22 \,\mu m$ (Costar, Corning, NY, USA) and centrifuged at 10,500 rpm for 5 min in a microcentrifuge (Fisher Scientific™, accuspin 17, Waltham, MA, USA). Zeta potential measurements of the filtered sample were performed using a Zetasizer (NanoSeries ZS, Malvern Instruments, London, UK). All experiments were conducted in triplicate and repeated twice.

2.5. Lipid analysis by high performance liquid chromatography (HPLC)

HPLC was used to determine the concentration of each lipid in the pure and the mixed lipid systems before and after addition of MgCl₂ solution. The amount of lipid in solution before addition of the salt was determined because there might be small errors in weighing the sample, or incomplete dissolution of aggregates upon rehydration of the lipid thin film, or loss during vesicle extrusion or filtration prior to HPLC analysis. Extruded vesicles were pre-

pared as described above in the section on ζ -potential measurement. Afterwards, a 500 μ L sample was filtered in a centrifuge tube filter (Costar, Corning, NY, USA) with a pore size of 0.22 μ m and centrifuged at 10,500 rpm for 5 min. It was assumed that most of the vesicle population would easily pass through the filter as the size of the extruded vesicles was 160–200 nm whereas lipid-Mg aggregates, which are expected to be larger, would be trapped on the filter.

Filtrates were analyzed by HPLC (Nexera 2, Shimadzu[®], Columbia, MD, USA), In detail, OA and POPC were separated through a Kinetex 2.6 µm Biphenyl 100 Å column, 100 mm × 4.6 mm (Phenomenex[®], Torrance, CA, USA) using a mobile phase of acetonitrile (MeCN)/H₂O (80:20) at a flow rate of 1 mL min⁻¹ (Fig. EA-5a). The mobile phase was acidified with 0.1% trifluoroacetic acid. The UV detection wavelength was set at 201 nm using UV-Vis photodiode array detector (SPD-M30A, Shimadzu®, Columbia, MD, USA). The separation was carried out at 40 °C. The quantitation of OA and POPC was achieved by using a calibration curve. For this, a series of OA and POPC standards with known concentrations were prepared. The absolute amount in the injected volume of standard solution was plotted against the area under the peak. Both OA and POPC calibration curves were linear up to 5 mM, meaning that the Lambert-Beer law was followed. All experiments were conducted in triplicate and the entire experiment was repeated two times. The error is reported as the standard deviation of the triplicates. Quantitation of the DA content in mixed DA-DOH vesicles was similarly obtained.

3. RESULTS

3.1. Fatal magnesium concentration [Mg²⁺]_{fatal}

The [Mg²⁺]_{fatal} was estimated using different assays. As the magnesium concentration increases, vesicles are ruptured and the ratio of the fluorescence intensity of the excimer to the monomer $(I_{EXC}:I_{MON})$ decreases. The magnesium concentration at which the ratio of the fluorescence intensity of excimer to monomer (I_{EXC} : I_{MON}) reached a minimum was assigned as the $[Mg^{2+}]_{fatal}$ (Fig. 2). The critical aggregate concentration (CAC) of pure OA is ~ 0.02 to 0.2 mM (Chen and Szostak, 2004a; Teo et al., 2011; Budin et al., 2014) while the CAC of PLs is generally <0.025 μM (Buboltz and Feigenson, 2005), so vesicles are abundantly present at the present experimental condition of 2 mM total lipid concentration. In the pure OA system, the excimer/ monomer intensity peaks reached a minimum at $\sim 5 \text{ mM}$ MgCl₂ compared to the system without Mg²⁺, so this value was defined as the [Mg²⁺]_{fatal}. With increasing relative POPC content in the mixed lipid vesicles, the minimum $I_{\rm EXC}{:}I_{\rm MON}$ ratio increased to \sim 17–20 mM for OA-POPC (10:1), 25-30 mM for OA-POPC (5:1), and was undetectable up to 40 mM MgCl₂ for OA-POPC (3:1), OA-POPC (1:1), and pure POPC (Fig. 2). Thus, the [Mg²⁺]_{fatal} drastically shifted to higher concentrations as the relative OA-POPC ratio decreased (Table 1). The effect of the vesicle size on the fluorescence was also examined. The results

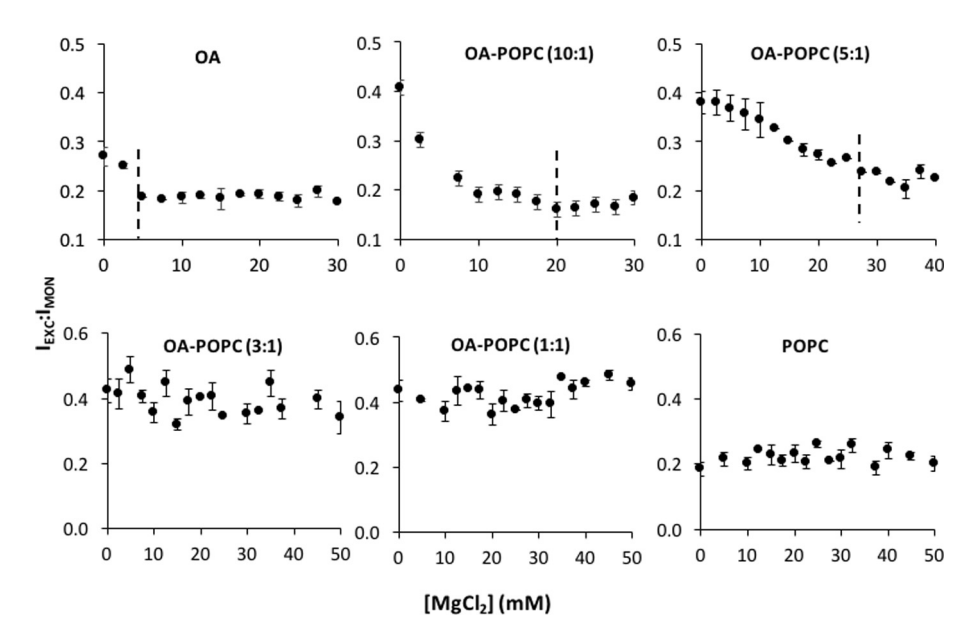


Fig. 2. Fatal magnesium concentration for various lipid systems determined by the naphthopyrene fluorescence assay. Ratio of the 465 nm NP excimer to the 390 nm monomer peak intensity as a function of MgCl₂ concentration determined 1 h after addition of MgCl₂ to the vesicle suspension. The vertical dashed line indicates the $[{\rm Mg}^{2^+}]_{\rm fatal}$; not detected for OA-POPC (3:1, 1:1) and POPC systems. [Total lipid] = 2 mM, pH = 8.5. Square brackets denote concentration. Error bars represent the standard deviation of measurements on triplicate samples.

Table 1 A compilation of $[Mg^{2+}]_{fatal}$ (mM) determined by various assays for pure and mixed lipid vesicle systems. [Total lipid] = 2 mM, pH = 8.5. Square brackets here and in subsequent tables denote concentration.

Assay	OA	OA-POPC (10:1)	OA-POPC (5:1)	OA-POPC (3:1)	OA-POPC (1:1)	POPC
NP-F ¹	5.0	17–20	25-30	ND	ND	ND
DLS ² -size	3.5	20	25	ND	ND	ND

¹ Naphthopyrene fluorescence.

showed a similar [Mg²⁺]_{fatal} values as for non-extruded vesicles (Fig. EA-1c).

If the effect of increasing Mg²⁺ concentration is to totally rupture the vesicles and cause aggregation of the lipids, then one might expect to see a concomitant increase in particle size from vesicles to aggregates, which can be determined by DLS (Fig. 3). Unilamellar and monodisperse vesicles prepared by extrusion through a 200 nm polycarbonate membrane were found to be $\sim 160-200 \text{ nm}$ (Fig. EA-2). Increase in particle size above 200 nm was taken to indicate the presence of both vesicles and aggregates as confirmed by phase contrast microscopy (Fig. EA-3). The magnesium concentration at which the particle diameter increased above 300 nm after addition of Mg²⁺ was assigned as the [Mg²⁺]_{fatal} as determined by DLS (Fig. 3, Table 1). For instance, it was found that 3.5 mM Mg²⁺ was needed to disrupt OA vesicles, whereas an eightfold greater amount of Mg²⁺ was needed to show disruptive effects on the OA-POPC (5:1) mixed system. A [Mg²⁺]_{fatal} was not detected for OA-POPC (3:1, 1:1) and pure POPC systems.

The substantial increase in the stability of mixed OA-POPC and POPC vesicles compared to pure OA vesicles was also confirmed by phase contrast microscopy

(Fig. EA-3). Note that most of the vesicles are below the resolution limit of the miscroscope. Even so, some stable vesicles >800 nm were observed in all the lipid systems in the absence of MgCl₂. For pure OA, lipid crystals appeared following the addition of $\sim 2 \text{ mM MgCl}_2$, but vesicles continued to coexist. The microscopy results remind us that the lipid systems consist of different phases in equilbrium with each other under different solution conditions. Thus, a small fraction of aggregates might still be present even at magnesium concentrations below fatal. In the pure OA system predominantly vesicles were observed at [Mg²⁺] <5 mM, and crystals of OA were observed at higher Mg²⁺ concentrations (Fig. EA-3). In the OA-POPC (3:1) system at 40 mM MgCl₂, some lipid-Mg²⁺ aggregates were observed in addition to vesicles. In the case of OA-POPC (1:1) and POPC systems, predominantly vesicles were seen up to 40 mM MgCl₂.

Results from fluorescence spectroscopy, particle size measurement experiments and phase contrast microscopy all demonstrated that mixed membranes with relatively higher POPC content display greater robustness towards magnesium and the quantitative values of the fatal magnesium concentrations determined by the various assays were consistent (Table 1).

² Particle size by DLS; ND: Not Detected (see text for details).

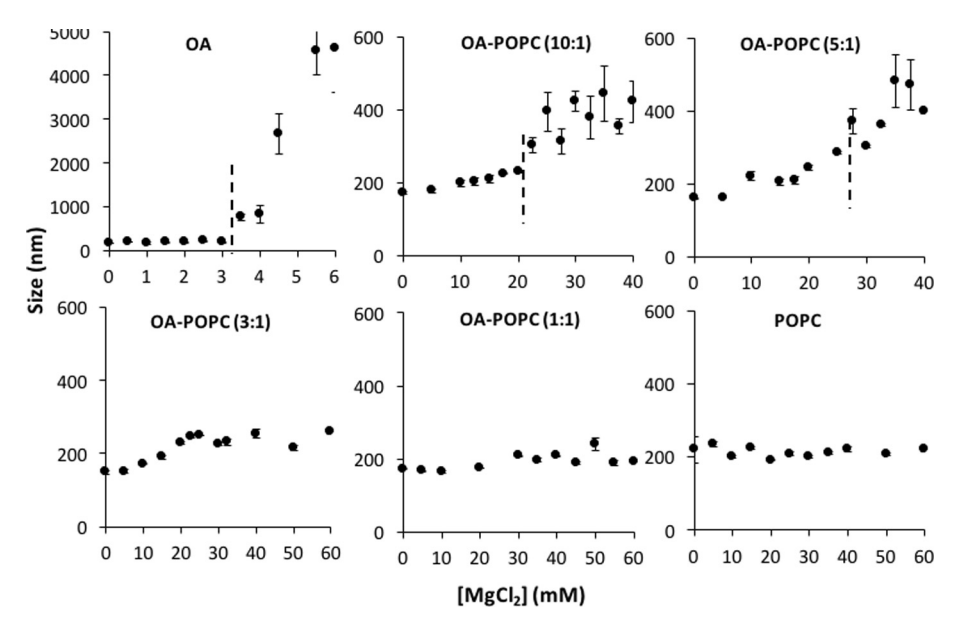


Fig. 3. The particle diameter (nm) of various lipid systems prepared as extruded vesicles as a function of the added $MgCl_2$ concentration. The vertical dashed line indicates the $[Mg^{2+}]_{fatal}$. A $[Mg^{2+}]_{fatal}$ could not be detected for OA-POPC (3:1, 1:1) and POPC systems. [Total lipid] = 2 mM, pH = 8.5. Square brackets denote concentration. Error bars represent the standard deviation of measurements on duplicate samples.

In addition to determining the $[Mg^{2+}]_{fatal}$ at [total lipid] = 2 mM, lower lipid concentrations of 0.25, 0.5, and 1 mM were also examined for all vesicle systems. For a given OA-POPC ratio, vesicles were more resistant to Mg^{2+} ions as the total lipid concentration increased (Table EA-2). Our results emphasize the caveat that, when citing fatal magnesium concentrations, the corresponding total lipid concentration should also be specified. The results above relate to estimates of membrane stability at a fixed time point after the addition of $MgCl_2$.

3.2. Vesicle membrane permeability

We next examined the response of the various vesicle systems to Mg²⁺ over time by determining changes in membrane integrity (permeability). The retention of an enclosed molecule is an important aspect of a stable membrane for the survival of a model protocell; yet some mass-exchange with the extracellular environment is required for maintenance.

Vesicles in all the lipid systems were nearly impermeable to calcein in the absence of MgCl₂ (Fig. 4, black curves), which is known previously for OA and POPC (Mansy et al., 2008; Sahai et al., 2017). The presence of only 5 mM MgCl₂ was able to completely disrupt pure OA vesicles within a few minutes (Fig. 4). For the OA-POPC (10:1) system, the curve at [Mg²⁺] = 5 mM showed a small initial decrease in encapsulation within the first 10 min, then increased back up to about 100% within the first 30 min, followed subsequently by a gradual decrease and reached steady state by 50 min. Similar trends were observed at the higher magnesium concentrations, but the changes were more dramatic. At the higher Mg²⁺ concentrations, 20% of the calcein had leaked out in the first 10 min and the vesicles were totally ruptured by 20 min. The percentage of encap-

sulated calcein seemed to increase and reached steady state by about 50 min. As discussed above, the apparent increase in encapsulation can be explained by the fact that after leaking out, calcein binds strongly to extra-vesicular Mg^{2+} and is re-quenched, so the fluorescence intensity decreases again. In summary, the $[\mathrm{Mg}^{2+}]_{\mathrm{fatal}}$ for the OA-POPC (10:1) system is greater than that of the pure OA system for up to at least 6 h.

The OA-POPC (5:1) system behaved similarly to the (10:1) system except that the apparent encapsulation was \geq 100% for the course of the experiment at [Mg²⁺] = 5 mM. The apparently >100% encapsulation suggests that the vesicles are leaky but have not ruptured. The curves at [Mg²⁺] = 20 mM and 30 mM were very similar, and the minimum percentage of encapsulation achieved at these concentrations was marginally more than in the presence of 40 mM MgCl₂.

The kinetics of apparent encapsulation in the OA-POPC (3:1), (1:1), and pure POPC systems were similar to each other in that the values were >100% at all time points indicating that the vesicles remained intact, though leaky; and the leaked-out calcein was re-quenched by binding to Mg²⁺ outside the vesicles. Secondly, for each lipid system, the apparent encapsulation of >100\% was maximum at the highest MgCl₂ concentration and decreased as magnesium concentration decreased. This indicates that membranes were the most leaky at the highest magnesium concentration though they were not ruptured entirely. It was observed in the OA-POPC (3:1) system, that the curves for 5 and 20 mM Mg were nearly identical and were separated from the 30 and 40 mM curves, which were similar to each other. By OA-POPC (1:1), the situation had progressed to 20 and 30 mM being almost identical whereas 40 mM was separate, and for pure POPC the 5, 20 and 30 mM curve were all very close while the 40 mM curve

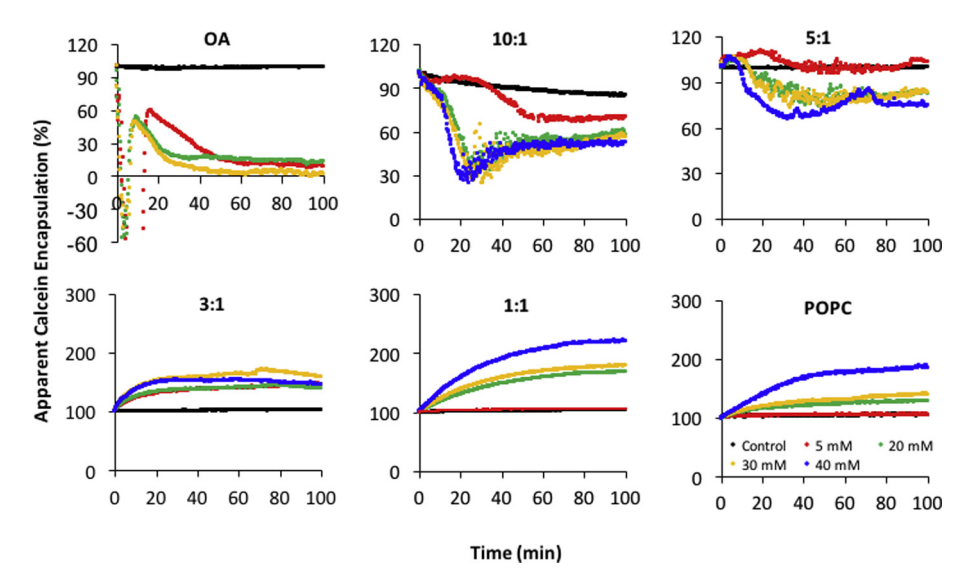


Fig. 4. Kinetics of apparent calcein leakage from various lipid systems at different concentrations of MgCl₂. The red, green, yellow and blue curves represent [MgCl₂] = 5, 20, 30 and 40 mM, respectively. Error bars obtained on duplicate samples are not shown for clarity. (For interpretation of the references to color in this figure legend, the reader is referred to the web version of this article.)

was still separate. The convergence of the apparent encapsulation curves obtained at lower and higher magnesium concentrations as the OA-POPC ratio decreases also indicates increasingly robust vesicles. In summary, the results of the above experiments show that the vesicles are more immune to Mg²⁺ as their POPC content increases. Finally, for some systems such as OA-POPC (1:1), (3:1) and (5:1), and even for (10:1) at low magnesium concentration, some leakage occurs without disrupting the vesicles completely, thus providing a semi-permeable membrane.

3.3. Lipid quantitation

In subsequent experiments, we quantitatively determined the concentration of OA and POPC in the membranes before and after their interaction with Mg²⁺ ions (Table 2, Fig. 5). When mixed lipid vesicles are prepared, it is always assumed that the lipid concentrations in the vesicles are the same as in the bulk mixing ratio. We first tested this assumption by determining OA and POPC concentrations by HPLC analysis in each lipid system in the absence of Mg²⁺. Small variations were found between the assumed bulk concentrations and the actual concentrations (Table 2). For example, the pure OA system was supposed to contain 2 mM total lipid, but it actually contained 1.5 mM OA and the OA-POPC (10:1) system actually had a ratio of 10.9:1. These variations could be attributed to human error during sample preparation as well as some lipid loss due to incomplete dissolution of lipid aggregates and removal of these aggregates during the extrusion and/ or filtration steps prior to HPLC analysis. After 1 h of interaction with 5 mM Mg²⁺ in the pure OA system, almost no OA was detected indicating that nearly all the OA was

In the case of the assumed (10:1) OA-POPC system, at $5 \text{ mM} \text{ MgCl}_2$ which is below the $[\text{Mg}^{2+}]_{\text{fatal}}$, only,

0.67 mM OA and 0.15 mM POPC were left in the vesicles. This indicated a dramatic drop in the OA-POPC ratio down to $\sim 4.5:1$ compared to the actual initial ratio of 10.9:1. At \sim 30 mM MgCl₂, which is near [Mg²⁺]_{fatal}, only 0.06 mM OA and 0.04 mM POPC remained in the filtrate as compared to the starting values of 1.74 mM OA and 0.16 mM POPC (Table 2, Fig. EA-5b and Table EA-3). Since the CAC of OA is ~ 0.02 to 0.2 mM, this remaining OA concentration of 0.06 mM would be insufficient for the formation of OA vesicles. About 0.04 mM POPC also remains, which is greater than its CAC <0.025 μM, so any vesicles present would be predominantly POPC in composition. This inference is also consistent with the observation, that the absolute concentration of OA in the vesicles decreases significantly whereas POPC concentration decreases only slightly. This behavior suggests that Mg²⁺ binds more strongly to the negatively-charged OA headgroup than the zwitterionic PC headgroup. Nonetheless, some binding of Mg²⁺ to the phosphate moiety of PC does occur and may still abstract some POPC at the higher magnesium concentrations (Table 2). The binding of Mg²⁺ to POPC is also reflected in the ζ-potential values measured for vesicles in the presence of magnesium (Table EA-4). For the pure POPC system, the ζ -potential is close to 0 mV at the lower magnesium concentrations but becomes positive above $[Mg^{2+}] = 30 \text{ mM}$; and for the mixed lipid systems, the ζ -potential values are close to zero above [Mg²⁺]_{fatal}. This suggests that magnesium can still bind to POPC, but removing it from the membrane is far less efficient than for OA.

Similar behavior was also observed for the nominal (5:1), (3:1) and (1:1) systems. In each case, the actual OA-POPC ratio was much lower than the bulk lipid mixing values. Indeed, the relative enrichment of the vesicles was even reversed for some systems such as the nominal (1:1) system at 30 mM and 40 mM MgCl₂ where the ratio evolved to

Table 2 Concentration and ratio of OA and POPC (mM) in pure and mixed vesicles after 1 h interaction with MgCl₂. Error bars, calculated as the standard deviation of triplicate samples, were within ± 0.04 mM. [Total lipid] = 2 mM, pH = 8.5.

MgCl ₂ (mM)	Lipid	OA	OA-POPC (10:1)	OA-POPC (5:1)	OA-POPC (3:1)	OA-POPC (1:1)	POPC
0	OA	1.5	1.74	1.56	1.33	0.93	_
	POPC	_	0.16	0.33	0.46	0.96	1.99
	Ratio	_	10.9:1	4.7:1	2.9:1	1:1	
5	OA	_	0.67	0.82	0.61	0.77	_
	POPC	_	0.15	0.31	0.41	0.96	_
	Ratio	No vesicles	4.5:1	2.7:1	1.5:1	0.8:1	
20	OA	_	0.23	0.51	0.54	0.6	_
	POPC	_	0.1	0.21	0.36	0.91	1.94
	Ratio		2.3:1	2.4:1	1.5:1	0.7:1	
30	OA	_	0.06	0.19	0.38	0.41	_
	POPC	_	0.04	0.12	0.29	0.78	_
	Ratio		1.5:1 ^a	1.6:1 ^a	1.3:1	0.5:1	
40	OA	_	_	0.03	0.38	0.4	_
	POPC	_	_	0.12	0.27	0.86	1.9
	Ratio			1.6:1 ^a	1.4:1	0.5:1	

^a Some vesicles exist, expected to be predominantly POPC in composition.

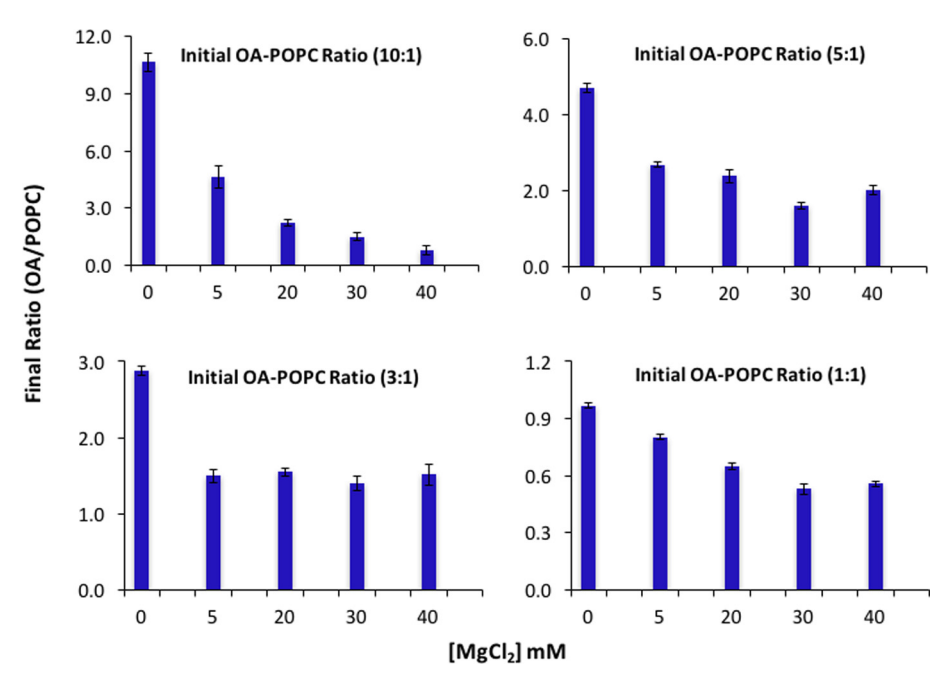


Fig. 5. Relative amount of OA-POPC in various mixed OA-POPC vesicle systems in the presence of $MgCl_2$ as determined by HPLC. [Total lipid] = 2 mM, pH = 8.5. Square brackets denote concentration. Error bars represent the standard deviation of measurements on triplicate samples.

0.5:1. These results unambiguously showed that there was a preferential selection of one lipid (OA) over another (POPC) by Mg^{2+} in the mixed lipid systems. Therefore, stable vesicles with a higher POPC content than initial were present below the $[Mg^{2+}]_{fatal}$.

In the nominal 10:1 system at 20 mM MgCl₂ the actual OA-POPC ratio of 2.3:1 compares well with the actual ratio of 2.7:1 in the nominal 5:1 system at 5 mM MgCl₂. Similarly, in the nominal 10:1 and nominal 5:1 systems at 30 mM, the actual ratios of 1.5:1 and 1.6, respectively, are

like the actual ratio of 1.5:1 in the nominal 3:1 system at all magnesium concentrations. Thus, even a small amount of POPC in the initial mixed lipid system when exposed to increasing Mg²⁺ concentrations, results in evolution towards POPC-rich membranes and, hence, more robust.

3.4. Mixed DA-DOH vesicles

It has been proposed that the most primitive protocells would have possessed membranes composed of short chain

fatty acids ($C \le 10$). Decanol does not form vesicles by itself but mixtures of DA-DOH have been widely studied (e.g., Apel et al., 2002; Monnard and Deamer, 2002; Sahai et al., 2017). The fatal concentrations of Mg²⁺ and Ca²⁺ for mixed DA-DOH (1:1 and 2:1) and pure DA vesicles were determined by DLS and fluorescence as described above for OA-POPC systems. As expected, higher fatal concentrations of Mg^{2+} (7–10 mM) and Ca^{2+} (≤ 5 mM) were found for the DA-DOH (1:1 and 2:1) systems than for pure DA vesicles $([Mg^{2+}]_{fatal} \sim 1$ to 1.5 mM and $[Ca^{2+}]_{fatal} \sim 1 \text{ mM}$), and the fatal concentrations for all DA-DOH systems were much smaller than for OA-POPC system. These results confirmed previous work, that (i) DA stabilizes mixed DOH vesicles compared to pure DOH, which is not vesice-forming; (ii) membranes are more susceptible to Ca²⁺ than to Mg²; and (iii) DA-DOH are less stable than OA-POPC (e.g., Apel et al., 2002; Monnard and Deamer, 2002; Mansy et al., 2008; Sahai et al., 2017).

The DA concentration in mixed DA-DOH (1:1 and 2:1) vesicles after 1 h exposure to MgCl₂ and CaCl₂ solutions of various concentrations was determined by HPLC. The results showed that both Mg²⁺ and Ca²⁺ can selectively abstract DA from mixed DA-DOH vesicles at concentrations of ~ 5 to 10 mM, and the effect of Ca²⁺ is more pronounced as reflected in the very low concentrations (Fig. EA-6). Thus, both cations were was able to shift the vesicle composition towards relative DOH enrichment.

4. DISCUSSION

The results of the above experiments show that the Mg²⁺-tolerance of the vesicles increases with increasing POPC content of the vesicle and increasing total lipid concentration.

4.1. Mechanisms for Mg²⁺-immunity

We propose at least two main mechanisms for the increased Mg^{2+} -tolerance of the mixed lipid vesicles with increasing POPC content and discuss data providing evidence for each hypothesis. The first is related to the net charge density of the vesicle and the second involves the ability of Mg^{2+} to bind to fatty acid head groups.

4.1.1. Vesicle charge density

The increasing immunity of the vesicles with increasing POPC content is likely an effect of the neutrally-charged

(zwitterionic) head group of POPC. As POPC content of the vesicles increases and the content of the negatively-charged head group (OA) decreases, the net negative charge density of the vesicles is expected to decrease. Consequently, more Mg^{2+} should be needed to disrupt the vesicles. This hypothesis was explored by determining the ζ -potential of the vesicles in the various lipid systems in the absence of magnesium (Table EA-4). Consistent with our expectation, ζ -potential was -88.6 mV for pure OA, -80.9 mV for OA-POPC (10:1), -75.7 mV for OA-POPC (5:1), -49.3 mV for OA-POPC (3:1), -52.6 mV for OA-POPC (1:1), and -0.1 mV for pure POPC.

4.1.2. Preferential selection of a lipid in a mixed membrane

We also hypothesize that increasing Mg²⁺-immunity is conferred on the vesicles as the OA-POPC ratio decreases, because Mg²⁺ preferentially binds to the negatively-charged OA head group and selectively abstracts it from the mixed lipid vesicle, thus relatively enriching the vesicle in POPC (Fig. 6, Table EA-3). Since POPC and PLs, in general, are known to form more impermeable membranes than fatty acids, the vesicles become increasingly more Mg²⁺-tolerant. Thus, we have shown an active role for Mg²⁺ whereby the vesicle composition was changed compared to the bulk mixing ratio of the lipids.

4.1.3. H⁺-bond and van der Waals bonds

In addition to charge-based arguments, the increasing stability conferred by POPC could partially be due to the formation of hydrogen bonds between the —NH₃⁺ moiety of the POPC head group and the —COO⁻ group of OA in the membrane bilayers (Cistola et al., 1988; Monnard et al., 2002; Budin and Szostak, 2011). Moreover, more favorable van der Waals interactions exist between the diacyl tails of a PL molecule and the monoacyl tail of a fatty acid molecule than between the monoacyl chains of two fatty acid molecules. This increases the bilayer order (Silvius and Leventis, 1993) and hinders abstraction as PL content increases.

4.2. Effect of total lipid concentration

The increasing [Mg²⁺]_{fatal} with increasing total lipid concentration can be explained by considering the CAC of lipids, which is the minimum concentration needed for the formation of micelles or vesicles. Below the CAC, lipid monomers exist, whereas vesicles and some

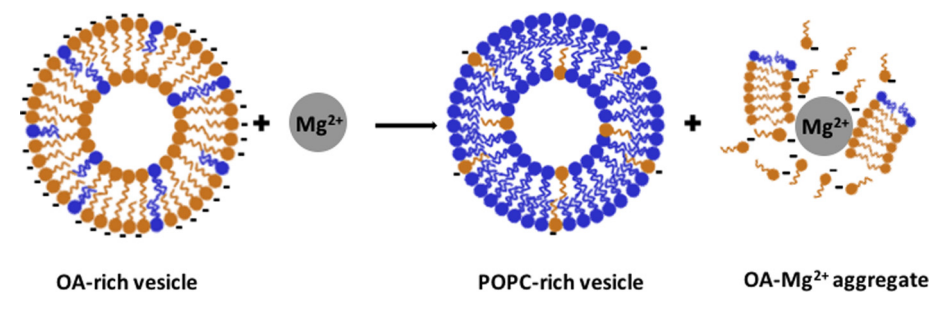


Fig. 6. Schematic of Mg^{2+} interaction with mixed lipid vesicles. The ratio of OA-POPC significantly decreases after the addition of $MgCl_2$ because Mg^{2+} preferentially binds to and removes OA.

micelles predominate above the CAC. As concentration increases above the CAC, the relative ratio of vesicles to micelles increases (Budin et al., 2012). In the present experiments, all the concentrations (0.25–2 mM) were above the CAC, but as concentration was decreased below 2 mM, the vesicle to micelle ratio decreased. Micelles are smaller than vesicles resulting in a relatively higher charge density and, hence, less magnesium is required to aggregate the lipids and remove them from solution at a given OA-POPC ratio.

4.3. Comparison with other lipid systems

The effect of divalent cations on phosphoserine (PS)-PC membranes prepared as vesicles or as supported lipid bilayers is worth comparing with our OA-PC system. We have shown that Mg²⁺ can bind to and abstract fatty acids from membranes because monoacyl chain fatty acids are highly mobile. Ca^{2+} , Mg^{2+} , Zn^{2+} and Ni^{2+} may bind to the negatively-charged head group of PS in a mixed PS-PC membrane without disrupting the bilayer structure, presumably because of the stronger diacyl chain interactions in PLs compared to OA and DA in the present study (Lau et al., 2006; Monson et al., 2012; Cong et al., 2015). Even the more strongly binding Cu²⁺ ion, which forms a Cu-PS₂ complex in a cis conformation (Kusler et al., 2016) did not disrupt a mixed PS-PC supported lipid bilayer at low ion concentrations (1 pM-0.1 mM) (Monson et al., 2012; Cong et al., 2015). However, vesicles of PS-PC may be disrupted at very high Cu²⁺ concentrations (0.1 M) but selective lipid abstraction was not discussed by those authors (Lau et al., 2006). Thus, the binding of Mg²⁺ to OA and the selective abstraction of OA from mixed OA-POPC vesicles seems to be unique or, at least, is reported for the first time.

We have demonstrated above that both Mg²⁺ and Ca²⁺ can selectively abstract DA from mixed DA- vesicles thus relatively depleting the vesicle in DA, and that Ca²⁺ is even more fatal than Mg²⁺. Two conclusions may be drawn from these results. First, the ability of these divalent cations to selectively abstract negatively charged lipid from mixed lipid vesicles is generally applicable over a wide range of lipid types. In the case of DA-DOH vesicles, for a given initial DA-DOH ratio, removal of DA would tend to destabilize the resulting vesicle by relatively enriching it in DOH, which does not form vesicles on its own. In contrast, removal of OA from each OA-POPC system makes the resulting vesicles more stable than before exposure to Mg²⁺. Thus, selective removal of negatively charged lipids stabilizes mixed vesicle systems when the other lipid is a more stable vesicle-former. Secondly, the results obtained on DA-DOH vesicles in the presence of Mg^{2+} and Ca^{2+} can be compared to results showing the ability of Cu^{2+} to disrupt vesicles at very high concentrations. The Ca²⁺ ion is less strongly hydrated than is Mg²⁺, so it is easier to desolvate Ca²⁺ and bind it to the negatively charged head group of DA compared to Mg²⁺. The Cu²⁺ ion is strongly hydrated but, at high enough concentrations, Cu2+ presumably forms enough complexes with PS to be able to abstract it from the vesicle.

4.4. Mg²⁺ as an environmental selection pressure for membrane evolution

The above results demonstrate that Mg²⁺ acts as an environmental selection pressure for the evolution of membranes from pure fatty acid to mixed fatty acid-PL and, eventually, pure PL membranes. Interestingly, the effect of Mg²⁺ as a selection pressure is the most dramatic at the largest OA-POPC (10:1) ratio, *i.e.*, for the most model system representing the more primitive protocell membrane. Thus, 97% OA was abstracted from the nominal (10:1) system whereas only 66% OA was abstracted from the nominal (1:1) system at 30 mM MgCl₂ (Table EA-2). In summary, the present HPLC results provide a unique mechanism for membrane evolution towards stable modern PL vesicles in the presence of Mg²⁺ salts.

A wide variety of geochemical environments on ancient Earth including oceans, tidal pools, brackish estuarine lakes and inland lakes have been proposed as potential settings for the concentration and assembly of prebiotic precursor molecules for protocells. These environments reflect all possible ionic strengths, and magnesium and ferrous iron were probably ubiquitous because of leaching from minerals in komatiitic and tonalitic crustal rock. Komatiite and basaltic rocks are also known to exist on Mars and many of the solid moons of Jupiter and Saturn. Evidence for weathering and deposition of salts of Mg and other cations is widespread on Mars and may also be on other solid worlds. Mg²⁺ or Fe²⁺ are necessary to activate the ribozyme or ribosome, which initiates RNA replication and oneelectron transfer reactions (Adamala and Szostak, 2013; Hsiao et al., 2013). Therefore, it is plausible that mixed fatty acid and PL membranes might have supported ribozyme activation and the emergence of encapsulating and replicating RNA. The increased stability of mixed SCA-PL membranes in the presence of divalent cations would also help in the emergence and evolution of metabolic machinery such as a proton gradient (Hsiao et al., 2013; Lane, 2015) and self-reproducing catalysts for further PL synthesis (Hardy et al., 2015). Thus, Mg²⁺ and other divalent cations that are virtually ubiquitous in aqueous geoenvironments could have provided an environmental selection pressure required for primitive cells to evolve into more robust compartments. In such scenarios, the availability of prebiotically synthesized PL molecules would have been an important limiting factor on the rate of evolution of the lipid membranes towards PL-rich compositions.

5. CONCLUSIONS

In summary, the present results showed that mixed OA-POPC vesicle systems are significantly more tolerant against rupture by Mg²⁺ than vesicles composed of OA alone. It was also shown here that vesicles are stable while still being semi-permeable at specific ratios of OA-POPC and can survive even in the presence of high concentrations of magnesium at mildly alkaline pH conditions. From an origins-of-life perspective, these results suggest that even the earliest protocell membrane composed of mixtures of

predominantly fatty acids and only trace concentrations of PLs synthesized abiotically may have been viable under such solution conditions.

At least two mechanisms were identified for the increasing Mg²⁺-immunity of mixed fatty phosphatidylcholine vesicles including reduction in vesicle charge-density, and a unique, active role for Mg²⁺ in selectively binding OA and abstracting it from solution. Significantly, the latter effect was most dramatic at the highest OA-POPC ratios, which represent the most primitive membranes. Thus, the membrane composition of protocells could have evolved in the presence of a strongly-binding cations from the initial fatty acid composition towards more resistant PL-rich compartments, which offer several evolutionary advantages over fatty acid membranes.

ACKNOWLEDGMENTS

We acknowledge financial support provided by NSF EAR grant (EAR-1251479), the Simons Foundation Origins of Life Initiative award (290359), and "start-up" funds from the University of Akron – United States. We are grateful for the invaluable conversations with present and former members of the Sahai research group, and with Prof. David Deamer, University of California-Santa Cruz.

APPENDIX A. SUPPLEMENTARY MATERIAL

Supplementary data associated with this article can be found, in the online version, at https://doi.org/10.1016/j.gca.2017.11.034.

REFERENCES

- Adamala K. and Szostak J. W. (2013) Nonenzymatic templatedirected RNA synthesis inside model protocells. Science 342, 1098–1100.
- Albertsen A. N., Duffy C. D., Sutherland J. D. and Monnard P.-A. (2014) Self-assembly of phosphate amphiphiles in mixtures of prebiotically plausible surfactants. *Astrobiology* 14, 462–472.
- Almgren M., Grieser F. and Thomas J. K. (1979) Dynamic and static aspects of solubilization of neutral arenes in ionic micellar solutions. J. Am. Chem. Soc. 101, 279–291.
- Apel C. L., Deamer D. W. and Mautner M. N. (2002) Self-assembled vesicles of monocarboxylic acids and alcohols: conditions for stability and for the encapsulation of biopolymers. *Biochim. Biophys. Acta Biomembranes* 1559, 1–9.
- Berner E. K. and Berner R. A. (2012) Global Environment: Water, Air, and Geochemical Cycles. Princeton University Press, New Jersey.
- Black R. A., Blosser M. C., Stottrup B. L., Tavakley R., Deamer D. W. and Keller S. L. (2013) Nucleobases bind to and stabilize aggregates of a prebiotic amphiphile, providing a viable mechanism for the emergence of protocells. *Proc. Natl. Acad. Sci. U. S. A.* 110, 13272–13276.
- Buboltz J. T. and Feigenson G. W. (2005) Phospholipid solubility determined by equilibrium distribution between surface and bulk phases. *Langmuir* **21**, 6296–6301.
- Budin I. and Szostak J. W. (2011) Physical effects underlying the transition from primitive to modern cell membranes. *Proc. Natl. Acad. Sci. U. S. A.* 108, 5249–5254.

- Budin I., Debnath A. and Szostak J. W. (2012) Concentrationdriven growth of model protocell membranes. J. Am. Chem. Soc. 134, 20812–20819.
- Budin I., Prywes N., Zhang N. and Szostak J. W. (2014) Chain-length heterogeneity allows for the assembly of fatty acid vesicles in dilute solutions. *Biophys. J.* 107, 1582–1590.
- Chen I. A. and Szostak J. W. (2004a) Membrane growth can generate a transmembrane pH gradient in fatty acid vesicles. *Proc. Natl. Acad. Sci. U. S. A.* 101, 7965–7970.
- Chen I. A. and Szostak J. W. (2004b) A kinetic study of the growth of fatty acid vesicles. *Biophys. J.* 87, 988–998.
- Chen I. A., Salehi-Ashtiani K. and Szostak J. W. (2005) RNA catalysis in model protocell vesicles. J. Am. Chem. Soc. 127, 13213–13219.
- Cheng Z. and Luisi L. P. (2003) Coexistence and mutual competition of vesicles with different size distributions. *J. Phys. Chem. B* **107**, 10940–10945.
- Cistola D. P., Hamilton J. A., Jackson D. and Small D. M. (1988) Ionization and phase behavior of fatty acids in water: application of the Gibbs phase rule. *Biochemistry* **27**, 1881–1888.
- Cong X., Poyton M. F., Baxter A. J., Pullanchery S. and Cremer P. S. (2015) Unquenchable surface potential dramatically enhances Cu²⁺ binding to phosphatidylserine lipids. *J. Am. Chem. Soc.* 137, 7785–7792.
- Dalai P., Kaddour H. and Sahai N. (2016) Incubating life: prebiotic sources of organics for the origin of life. *Elements* 12, 401–406.
- Deamer D. W. and Oró J. (1980) Role of lipids in prebiotic structures. *Biosystems* 12, 167–175.
- Deamer D. W. and Pashley R. M. (1989) Amphiphilic components of the murchison carbonaceous chondrite surface-properties and membrane formation. *Orig. Life Evol. Biosph.* **19**, 21–38.
- Deamer D. W. (1992) Polycyclic aromatic hydrocarbons: primitive pigment systems in the prebiotic environment. *Adv. Space Res.* **12**, 183–189.
- Ferris J. P., Hill, Jr, A. R., Liu R. and Orgel L. E. (1996) Synthesis of long prebiotic oligomers on mineral surfaces. *Nature* **381**, 59–61.
- Fiore M., Madanamoothoo W., Berlioz-Barbier A., Maniti O., Girard-Egrot A., Bucheta R. and Strazewski P. (2017) Giant vesicles from rehydrated crude mixtures containing unexpected mixtures of amphiphiles formed under plausibly prebiotic conditions. *Org. Biomol. Chem.* 15, 4231–4240.
- Foustoukos D. I. (2004) Hydrocarbons in hydrothermal vent fluids: the role of chromium-bearing catalysts. *Science* **304**, 1002–1005.
- Furry J. W. (1985) Preparation, properties and applications of calcein in a highly pure form Ph. D. thesis. Iowa State Univ..
- Gebicki J. M. and Hicks M. (1976) Preparation and properties of vesicles enclosed by fatty acid membranes. *Chem. Phys. Lipids* **16**, 142–160.
- Groen J., Deamer D. W., Kros A. and Ehrenfreund P. (2012) Polycyclic aromatic hydrocarbons as plausible prebiotic membrane components. *Orig. Life Evol. Biosph.* **42**, 295–306.
- Hardy M. D., Yang J., Selimkhanov J., Cole C. M., Tsimring L. S. and Devaraj N. K. (2015) Self-reproducing catalyst drives repeated phospholipid synthesis and membrane growth. *Proc. Natl. Acad. Sci. U. S. A.* 112, 8187–8192.
- Hargreaves W. R., Mulvihill S. J. and Deamer D. (1977) Synthesis of phospholipids and membranes in prebiotic conditions. *Nature* 266, 78–80.
- Hargreaves W. R. and Deamer D. W. (1978) Liposomes from ionic, single-chain amphiphiles. *Biochemistry* 17, 3759–3768.

- Hsiao C., Chou I.-C., Okafor C. D., Bowman J. C., O'Neill E. B., Athavale S. S., Petrov A. S., Hud N. V., Wartell R. M., Harvey S. C. and Williams L. D. (2013) RNA with iron(II) as a cofactor catalyses electron transfer. *Nat. Chem.* 5, 525–528.
- Joshi P. C., Aldersley M. F., Delano J. W. and Ferris J. P. (2009) Mechanism of montmorillonite catalysis in the formation of RNA oligomers. J. Am. Chem. Soc. 131, 13369–13374.
- Joshi P. C. and Aldersley M. F. (2013) Significance of mineral salts in prebiotic RNA synthesis catalyzed by montmorillonite. *J. Mol. Evol.* 76, 371–379.
- Kee T. P. and Monnard P.-A. (2016) On the emergence of a protometabolism and the assembly of early protocells. *Elements* 12, 419–424.
- Komiya M., Shimoyama A. and Harada K. (1993) Examination of organic compounds from insoluble organic matter isolated from some Antarctic carbonaceous chondrites by heating experiments. *Geochim. Cosmochim. Acta* 57, 907–914.
- Kusler K., Odoh S. O., Silakov A., Poyton M. F., Pullanchery S., Cremer P. S. and Gagliardi L. (2016) What is the preferred conformation of phosphatidylserine—copper(II) complexes: a combined theoretical and experimental investigation. *J. Phys. Chem. B* 120, 12883–12889.
- Lane N. (2015) The Vital Question: Energy, Evolution, and the Origins of Complex Life. W. W. Norton & Company, New York.
- Lau T.-L., Ambroggio E. E., Tew D. J., Cappai R., Masters C. L., Fidelio G. D., Barnham K. J. and Separovic F. (2006) Amyloidbeta peptide disruption of lipid membranes and the effect of metal ions. J. Mol. Biol. 356, 759–770.
- Lawless J. G. and Yuen G. U. (1979) Quantitation of monocarboxylic acids in the Murchison carbonaceous meteorite. *Nature* 282, 431–454.
- Maheen G., Tian G., Wang Y., He C., Shi Z., Yuan H. and Feng S. (2010) Resolving the enigma of prebiotic C-O-P bond formation: prebiotic hydrothermal synthesis of important biological phosphate esters. *Heteroat. Chem.* **21**, 161–167.
- Mansy S. S. and Szostak J. W. (2008) Thermostability of model protocell membranes. *Proc. Natl. Acad. Sci. U. S. A.* 105, 13351–13355.
- Mansy S. S., Schrum J. P., Krishnamurthy M., Tobé S., Treco D. A. and Szostak J. W. (2008) Template-directed synthesis of a genetic polymer in a model protocell. *Nature* 454, 122–125.
- Mautner M., Leonard R. L. and Deamer D. W. (1995) Meteorite organics in planetary environments: hydrothermal release, surface activity and microbial utilization. *Planet. Space Sci.* 43, 139–140.
- McCollom T. M., Ritter G. and Simoneit B. R. T. (1999) Lipid synthesis under hydrothermal conditions by Fischer-Tropsch-Type reactions. *Orig. Life Evol. Biosph.* 29, 153–166.
- Monnard P.-A. and Deamer D. W. (2002) Membrane self-assembly processes: Steps toward the first cellular life. *Anat. Rec.* 268, 196–207.
- Monnard P.-A., Apel C. L., Kanavarioti A. and Deamer D. W. (2002) Influence of ionic inorganic solutes on self-assembly and polymerization processes related to early forms of life: implications for a prebiotic aqueous medium. *Astrobiology* **2**, 139–152.
- Monson C. F., Cong X., Robison A. D., Pace H. P., Liu C., Poyton M. F. and Cremer P. S. (2012) Phosphatidylserine reversibly

- binds Cu²⁺ with extremely high affinity. *J. Am. Chem. Soc.* **134**, 7773–7779.
- Namani T. and Deamer D. W. (2008) Stability of model membranes in extreme environments. *Orig. Life Evol. Biosph.* 38, 329–341.
- Nooner D. W. and Oró J. (1979) Synthesis of fatty acids by a closed system Fischer-Tropsch process. Adv. Chem. 178, 159– 171.
- Oró J., Miller S. L. and Lazcano A. (1990) The origin and early evolution of life on Earth. *Annu. Rev. Earth Planet. Sci.* 18, 317.
- Patel B. H., Percivalle C., Ritson D. J., Duffy C. D. and Sutherland J. D. (2015) Common origins of RNA, protein and lipid precursors in a cyanosulfidic protometabolism. *Nat. Chem.* 7, 301–307.
- Rao M., Eichberg J. and Oró J. (1982) Synthesis of phosphatidylcholine under possible primitive earth conditions. *J. Mol. Evol.* 18, 196–202.
- Rao M., Eichberg J. and Oró J. (1987) Synthesis of phosphatidylethanolamine under possible primitive earth conditions. J. Mol. Evol. 25, 1–6.
- Rushdi A. I. and Simoneit B. R. T. (2001) Lipid formation by aqueous Fischer-Tropsch-type synthesis over a temperature range of 100 to 400 °C. *Orig. Life Evol. Biosph.* 31, 103–118.
- Russell M. J., Barge L. M., Bhartia R., Bocanegra D., Bracher P. J., Branscomb E., Kidd R., McGlynn S., Meier D. H., Nitschke W., Shibuya T., Vance S., White L. and Kanik I. (2014) The drive to life on wet and icy worlds. *Astrobiology* 14, 308–343.
- Sacerdote M. G. and Szostak J. W. (2005) Semipermeable lipid bilayers exhibit diastereoselectivity favoring ribose. *Proc. Natl. Acad. Sci. U. S. A.* 102, 6004–6008.
- Sahai N., Kaddour H., Dalai P., Wang Z., Bass G. and Gao M. (2017) Mineral surface chemistry and nanoparticle-aggregation control membrane self-assembly. Sci. Rep. 7, 43418. https://doi. org/10.1038/srep43418.
- Schenkman S., Araujo P. S., Dukman R., Quina F. H. and Chaimovich H. (1981) Effects of temperature and lipid composition on the serum albumin-induced aggregation and fusion of small unilamellar vesicles. *Biochim. Biophys. Acta Biomem*branes 649, 633–641.
- Silvius J. R. and Leventis R. (1993) Spontaneous interbilayer transfer of phospholipids: dependence on acyl chain composition. *Biochemistry* **32**, 13318–13326.
- Teo Y. Y., Misran M., Low K. H. and Zain S. M. (2011) Effect of unsaturation on the stability of C₁₈ polyunsaturated fatty acids vesicles suspension in aqueous solution. *Bull. Korean Chem.* Soc. 32, 59–64.
- Vanderkooi J. M. and Callis J. B. (1974) Pyrene. Probe of lateral diffusion in the hydrophobic region of membranes. *Biochemistry* 13, 4000–4006.
- Yuen G. U. and Kvenvolden K. A. (1973) Monocarboxylic acids in murray and murchison carbonaceous meteorites. *Nature* 246, 301–303.
- Zepik H. H., Rajamani S., Maurer and Deamer D. W. (2007) Oligomerization of thioglutamic acid: encapsulated reactions and lipid catalysis. *Orig. Life Evol. Biosph.* 37, 495–505.

Associate editor: Hailiang Dong